The Mutant *Escherichia coli* F112W Cyclophilin Binds Cyclosporin A in Nearly Identical Conformation as Human Cyclophilin[†,‡]

Jasna Fejzo, Felicia A. Etzkorn,[§] Robert T. Clubb,[∥] Yian Shi, Christopher T. Walsh, and Gerhard Wagner[*]

Department of Biological Chemistry and Molecular Pharmacology, Harvard Medical School, 240 Longwood Avenue, Boston, Massachusetts 02115

Received December 1, 1993; Revised Manuscript Received February 23, 1994[⊗]

ABSTRACT: The periplasmic *Escherichia coli* cyclophilin is distantly related to human cyclophilin (34% sequence identity). Peptidyl–prolyl isomerase activity, cyclosporin A binding, and inhibition of the calcium-dependent phosphatase calcineurin are compared for human and *E. coli* wild-type and mutant proteins. Like human cyclophilin, the *E. coli* protein is a *cis–trans* peptidyl–prolyl isomerase. However, while the human protein binds cyclosporin A tightly (K_d = 17 nM), the *E. coli* protein does not (K_d = 3.4 μM). The mutant F112W *E. coli* cyclophilin has enhanced cyclosporin binding (K_d = 170 nM). As for the human protein, the complex of the *E. coli* mutant with cyclosporin A inhibits calcineurin. Here we describe the structure at pH 6.2 of cyclosporin A bound to the mutant *E. coli* cyclophilin as solved with solution NMR methods. Despite the low overall sequence identity, the structure of the bound cyclosporin A is virtually identical in both proteins. To assess differences of the cyclosporin binding site, the solution structure of wild-type *E. coli* cyclophilin was compared with structures of uncomplexed human cyclophilin A and with cyclosporin bound. Despite the structural similarity of bound cyclosporin A, the architecture of the binding site in the *E. coli* protein is substantially different at the site most distant to tryptophan 121 (human sequence). This site is constructed by a five-residue insertion in a loop of the *E. coli* protein, replacing another loop in the human protein.

Subsequent to the discovery that calcineurin is the putative target of the immunosuppressive drug cyclosporin A (CsA)[1] (Liu et al., 1991b), much attention has focused on the roles of various isoforms of cyclophilin, the protein that binds and presents CsA. The cyclophilin proteins have two fascinating, but separable functions (Zydowsky et al., 1992): peptidyl–prolyl isomerase (PPIase) enzymatic activity (Fischer et al., 1989) and immunosuppressant cyclosporin A complexation for inhibition of calcineurin (CN) (Liu et al., 1991b). Previous mutagenesis studies have shown that the peptidyl–prolyl isomerase activity could be destroyed without loss of the ability to bind CsA at the PPIase active site or inhibit CN (Zydowsky et al., 1992). It has also been shown that cyclophilin selects from solution the rare conformer(s) of CsA required for calcineurin inhibition (Kofron et al., 1992); that is, it does not isomerize the 9,10 amide bond of bound CsA as had been previously proposed (Fesik et al., 1991). These two results clearly indicate that the PPIase activity of human cyclophilin A (hCyPA) is not relevant for immunosuppression and allow one to focus on the structure of the drug/immunophilin complex (Pflügl et al., 1993; Thériault et al., 1993). We have recently reported mutants of hCyPA away from the active site that either weaken or strengthen the ability of the CsA/hCyPA complex to serve as a noncompetitive inhibitor of calcineurin phosphatase activity (Etzkorn et al., 1994).

The X-ray structures of uncomplexed human cyclophilin (hCyP) (Ke et al., 1991; Ke, 1992), a tetrapeptide/hCyA complex (Kallen et al., 1991; Kallen & Walkinshaw, 1992), and a complex of hCyP with an Ala-Pro dipeptide (Ke et al., 1993) have been solved. A first model of the hCyP/CsA complex was based on both X-ray and NMR data (Spitzfaden et al., 1992; Fesik et al., 1992). Recently an X-ray structure of a decameric hCyP/CsA complex (Pflügl et al., 1993) has been determined. NMR structures of CsA when bound to hCyP have been reported independently by two groups (Weber et al., 1991; Fesik et al., 1991). It was found that the structure of the bound CsA was entirely different from the conformation of free CsA in chloroform solution (Kessler et al., 1990). A similar result was reported recently from studies of CsA bound to perdeuterated hCyP (Hsu & Armitage, 1992). In the latter study, it was shown that the nonimmunosuppressant MeAla-6 CsA analogue has an identical backbone conformation. While the NMR solution structure of the hCyP/CsA complex was presented earlier (Thériault et al., 1993), an NMR solution structure of an uncomplexed cyclophilin has only been solved recently for the *Escherichia coli* protein (Clubb et al., 1994).

The existence of several cloned isoforms of human cyclophilins, including the very distantly related *E. coli* periplasmic cyclophilin (34% identity) (Liu & Walsh, 1990), offers an opportunity to discover those features of the human protein which are critical to the immunosuppression process. The *E. coli* cyclophilin can be thought of as an ultimate mutant of human cyclophilin A, the immunosuppressive drug target, sharing PPIase activity and sequence similarity, but 500-fold poorer in CsA binding (Liu et al., 1991a). Previously, mutation of the eCyP at the site analogous to the single tryptophan 121

[†] This research was supported by the NIH (Grant GM 47467) and by the Keck Foundation.

[‡] Coordinates have been deposited in the Brookhaven Protein Data Bank under the file name 1CSA.

[*] Address correspondence to this author.

[§] Current address: Department of Chemistry, University of Virginia, Charlottesville, VA 22901.

[∥] Current address: National Institutes of Health, Bethesda, MD 20892.

[⊗] Abstract published in *Advance ACS Abstracts,* April 15, 1994.

[1] Abbreviations: CN, calcineurin; CsA, cyclosporin A; COSY, correlation spectroscopy; eCyP, *Escherichia coli* cyclophilin; hCyPA, human T cell cyclophilin isoform A; HMQC, heteronuclear multiple-quantum coherence; HSQC, heteronuclear single-quantum coherence; NMR, nuclear magnetic resonance; NOE, nuclear Overhauser enhancement; NOESY, two-dimensional nuclear Overhauser enhancement spectroscopy; PPIase, *cis–trans* peptidyl–prolyl isomerase; PSPase, protein serine phosphatase; rmsd, root mean square deviation; [U-^{13}C], uniformly ^{13}C enriched; [U-^{15}N], uniformly ^{15}N enriched.

0006-2960/94/0433-5711$04.50/0

in human cyclophilin, phenylalanine 112, produced an F112W protein with improved affinity for cyclosporin A (Liu et al., 1991a). Since the discovery of calcineurin as the putative target for the CyP/CsA drug complex (Liu et al., 1991b), we have tested the human cyclophilin A complementary mutant protein W121A as a presenter of CsA for inhibition of CN in a phosphatase enzyme assay. W121A was found to bind CsA about 17-fold weaker than wild type while completely losing the ability to inhibit CN (Zydowsky et al., 1992). Conversely, the *E. coli* F112W mutant gains 20-fold affinity for CsA (Liu et al., 1991a), and here we show that it becomes a CN inhibitor. We have now determined the structure of CsA bound to F112W and compared it with CsA bound to human cyclophilin. This work and ongoing studies on the complex of CsA with the F112W mutant CyP aim at a better understanding of the determinants of CsA/CyP interactions.

EXPERIMENTAL PROCEDURES

NMR Sample Preparation. The eCyP F112W mutant was overproduced and purified as described previously (Liu et al., 1991a). The protein was then exchanged into 50 mM sodium phosphate buffer (pH 6.2) and concentrated to 1 mM with a Centricon-3. For ^2H_2O NMR samples the protein was lyophilized and dissolved in ^2H_2O. The [U-^{13}C]CsA/F112W cyclophilin complex was prepared as previously desribed (Heald et al., 1990) by gently inverting a suspension of ~1.5 mol equiv of [U-^{13}C]CsA in a ^2H_2O solution of cyclophilin F112W at 4 °C for 24 h under argon. The excess CsA was removed by centrifugation. The [U-^{15}N]CsA/F112W cyclophilin complex was prepared in the same way starting from [U-^{15}N]CsA and an H_2O solution of cyclophilin F112W. The final concentration of both CsA/F112W cyclophilin complexes was 1 mM.

NMR Experiments. All the NMR spectra were recorded on a Bruker AMX600 spectrometer at 25 °C, unless otherwise stated. Heteronuclear correlation spectra were recorded with the pulse sequence of Bodenhausen and Ruben (1980) modified by addition of a spin-lock purge pulse (Otting & Wüthrich, 1988) to suppress all signals originating from protons not bound to a heterospin. The (^{13}C,^{1}H)HSQC spectrum was collected with 2048 real points in ω_2 and 512 real points in ω_1, with 80 scans and 4 dummy scans. The sweep width was 9615 Hz in ω_2 and 10 504 Hz in ω_1.

The ^{13}C(ω_1,ω_2) double-half-filtered NOESY spectrum was collected with a previously described pulse sequence (Otting & Wüthrich, 1990). The data set consisting of 512 by 1024 real points was acquired with 128 scans and 4 dummy scans. The sweep width was 9615 Hz in both ω_1 and ω_2. The ^{15}N(ω_2) half-filtered NOESY spectrum was collected using a pulse sequence with pulsed field gradients (Lee et al., 1993) on a Varian Unity 500 spectrometer equipped with shielded gradients. A data set of 256 × 1024 complex points was acquired with 192 scans and 4 dummy scans with the sweep width of 8000 Hz in both ω_1 and ω_2. The filter delays were set to 3.6 ms for ^{13}C-filtered and 5.5 ms for ^{15}N-filtered experiments. Heteronuclear decoupling was accomplished by a 180° proton pulse in the middle of t_1. The transmitter was offset to 42.9 ppm in the ^{13}C dimension and to 116 ppm in the ^{15}N dimension.

The 3D NOESY-HMQC spectrum (Fesik & Zuiderweg, 1988) was acquired with a mixing time of 50 ms. The data set was recorded as 54 (t_1) (complex) × 196 (t_2) (real) × 1024 (t_3) (real) points with 48 scans and 16 dummy scans and with spectral widths of 5490 Hz in ω_1 and 9615 Hz in both ω_2 and ω_3.

The HCCH-COSY spectrum (Bax et al., 1990) was recorded with 192 (t_1) (real) × 44 (t_2) (complex) × 1024 (t_3) (real) points with 32 scans and 4 dummy scans and with spectral widths of 9203 Hz in ω_1 and ω_3 and 4026 Hz in ω_2. The quantitative *J*-correlation spectrum was recorded with a pulse sequence recently described by Vuister and Bax (1993). A 2D version of the experiment was used to acquire a data set of 64 (t_1) (complex) × 1024 (t_2) (real) points with 256 scans and 4 dummy scans and with a spectral width of 10 000 Hz in both ω_1 and ω_2. In all heteronuclear experiments mentioned, heteronuclear decoupling in t_2 was accomplished using the GARP sequence. The NMR data were processed using the program Felix (Hare Research, Inc.).

Structure Calculations. Three-dimensional structures were calculated by a dynamical simulated annealing procedure (Nilges et al., 1988) in the BIOSYM NMR refine package (Insight II User Guide, version 2.1.0, Biosym Technologies, 1993). The starting structures for the calculations were generated by randomly assigning Cartesian coordinates to each atom. In stage 1, 1400 steps of minimization (time step of 1 fs) were applied at 1000 K. The force constants of the terms in the consistent valence force field (CVFF) and for NOE distance restraints were set to 0.001 kcal mol^{-1} Å^{-4}. The usual Lennard-Jones potential for van der Waals interaction was replaced with a purely repulsive quartic form with a force constant of 0.001 kcal mol^{-1} Å^{-4}. In stage 2, a series of 1.4-ps dynamics runs at 1000 K were performed, and after each 1.4 ps the internal force constant was multiplied by a factor of 1.43 until NOE restraint force constants reached 100 kcal mol^{-1} Å^{-2}. The van der Waals force constant was kept at 0.001 kcal mol^{-1} Å^{-4}. When the bond force constants reached 100 kcal mol^{-1} Å^{-2}, the van der Waals force constant was increased by a factor of 1.35 each 1.4 ps from its initial value of 0.001 kcal mol^{-1} Å^{-4} until it reached 0.25 kcal mol^{-1} Å^{-4}, which occurred 56 ps after the beginning of the dynamics run. In stage 3, 14-ps dynamics simulations were performed during which the temperature was cooled to 300 K. In stage 4, 100 steps of steepest descent followed by 500 steps of conjugated gradient restrained energy minimization were carried out. In the last stage, the structures were subjected to 100 steps of steepest descent and 1000 steps of conjugated gradient restrained energy minimization with a standard Lennard-Jones potential for the van der Waals interaction.

RESULTS

Cyclophilin Affinities. The wild-type and F112W eCyP proteins were overproduced, purified, and assayed for PPIase and CsA inhibition activities as described previously (Liu et al., 1991a). A new continuous assay developed in related work (Etzkorn et al., 1994) was used for measuring the inhibition of CN by the CyP/CsA complexes. The CsA inhibition data were fit to an equation for competitive inhibition (Zydowsky et al., 1992) to give K_i values instead of the previously reported IC_{50} values (Liu et al., 1991a). Wild-type *E. coli* CyP binds CsA at K_i = 3400 nM, while the mutant F112W has a binding constant of 170 nM (Table 1), a 20-fold improvement. The eCyP proteins were shown to have the same affinities for CsA after overnight incubation with the drug, indicating no slow-binding effects. However, an interesting observation was made that CsA stabilizes the enzymatic activity of the cyclophilins up to 500 nM CsA in the case of wild type and up to ca. 100 nM for the F112W mutant. At higher concentrations of the drug, inhibition takes over, and these data were used to assess inhibition constants for the preincubated proteins. In the CN inhibition assay,

Table 1: Comparison between Wild Type and Mutants of hCyP and eCyP of k_{cat}/K_m for the PPIase Activity and Dissociation Constants for CsA Binding to CyP and the CsA/Cyp Complex with Calcineurin

	k_{cat}/K_m (μM^{-1} s^{-1})	K_i(CsA) (nM)	K_i(CsA/CyP) (nM)
hCyPA			
WT	16	17 ± 2	270 ± 40
W121F[a]	9.2	490 ± 20	3150 ± 250
W121A[a]	1.4	290 ± 30	*b*
E. coli CyP			
WT	20	3400 ± 280	>5000
F112W	10	170 ± 20	1070 ± 70

[a] Etzkorn et al., 1994. [b] Not an inhibitor at ≤5 μM CsA.

the wild-type protein has a barely detectable effect on CN phosphatase activity, even up to 5 μM complex concentration, but the mutant has an inhibition constant of 1070 nM, only about 4-fold worse than human CyPA, K_i = 270 nM (Etzkorn et al., 1994), even though it binds CsA 10-fold less tightly than hCyPA. Thus the F112W mutant of eCyP was analyzed for the conformation of bound CsA.

NMR Assignments of CsA Bound to E. coli CyP F112W. Initial tentative assignments for the majority of the ^1H and ^{13}C resonances were obtained by a direct comparison of the two-dimensional heteronuclear single-quantum correlation (^{13}C,^1H) (HSQC) spectrum of cyclosporin bound to eCyP mutant F112W ([U-^{13}C]CsA F112W) (Figure 1) with the HSQC spectrum of cyclosporin bound to human cyclophilin hCyPA (Neri et al., 1991). The assignments were confirmed in a 3D HMQC-NOESY spectrum and in a doubly selected subspectrum of a double-half-filtered NOESY experiment, which contains all the intramolecular NOEs between ^{13}C-bound protons of CsA. CsA amide protons were assigned from a 2D NOESY spectrum in an H_2O solution of [U-^{15}N]-CsA bound to the eCyP mutant F112W. A gradient-enhanced $^{15}N(\omega_2)$ half-filtered NOESY spectrum (Lee et al., 1993) was used to analyze NOESY peaks to CsA amide protons. It selects for cross peaks to CsA amide proton lines along ω_2 (Figure 2). Sequential assignments obtained with $d_{\alpha N}$ and $d_{\alpha NQ}$ (where Q represents the CH_3 group for residues with methylated amide groups) connectivities were further confirmed by sequential NOE connectivities $d_{\beta N}$, $d_{\beta NQ}$, and d_{NQNQ} (Figure 2). Side-chain resonances of all CsA residues were assigned by analysis of (^{13}C,^1H)HSQC- and HMQC-NOESY spectra.

H^γ, H^δ, and H^ζ proton resonances in MeBmt-1 and the MeLeu-9 H^β resonance could not be assigned from either the (^{13}C,^1H)HSQC spectrum or the HMQC-NOESY spectrum. These resonances were also not observed in an HCCH-COSY spectrum which was used to check side-chain assignments. The list of CsA ^1H and ^{13}C chemical shift resonances is given in Table 2. Chemical shift differences between CsA bound to *E. coli* cyclophilin F112W and CsA bound to hCyPA are shown in Figure 3.

Structural Parameters for the Bound CsA. In the ^{13}C-resolved 3D NOE spectrum, NOEs were observed that originated from protons attached to the ^{13}C-labeled nuclei of

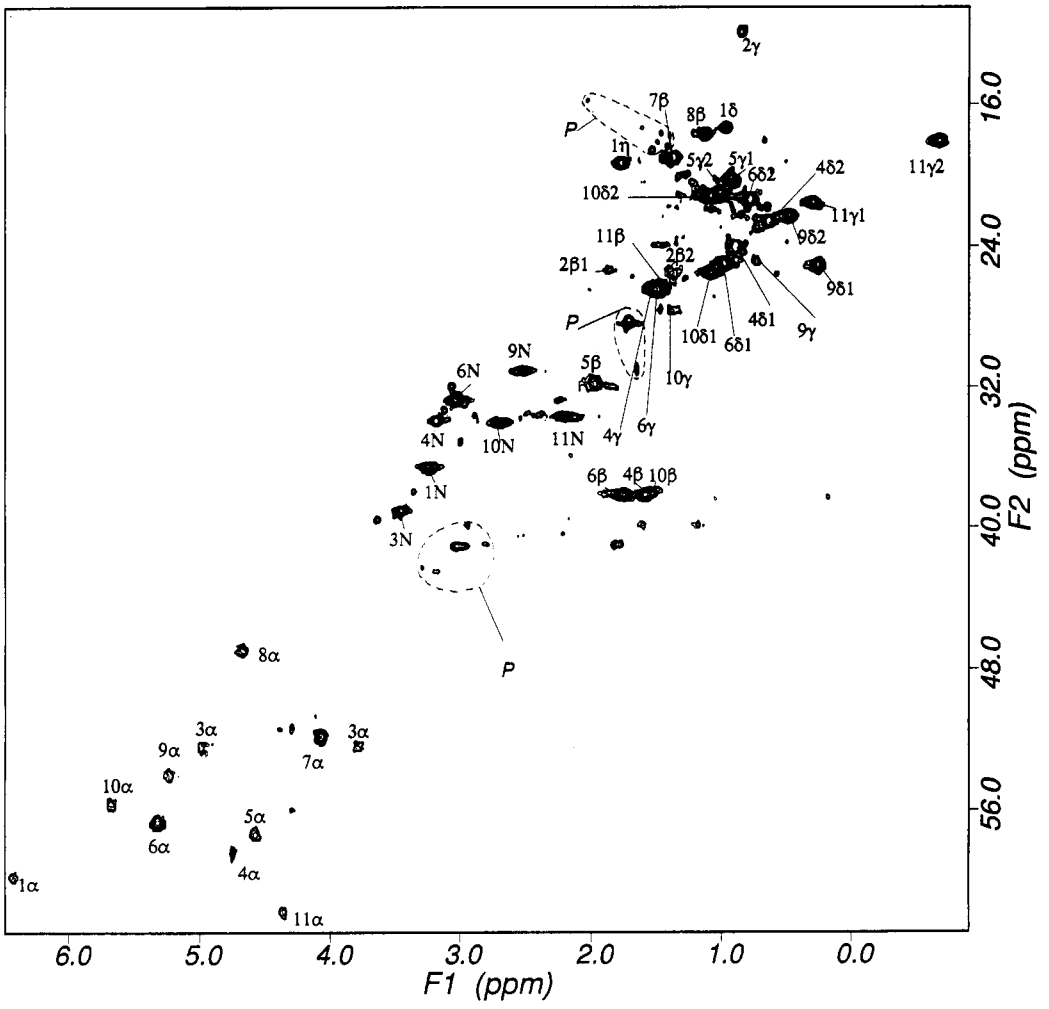

FIGURE 1: Contour plot of the HSQC spectrum of [U-^{13}C]CsA bound to unlabeled eCyP F112W. *P* indicates residual protein cross peaks (1 mM complex in 440 μL of D_2O, 50 mM sodium phosphate, and 0.04% sodium azide, pH* 6.2, 25 °C, ^1H frequency 600 MHz).

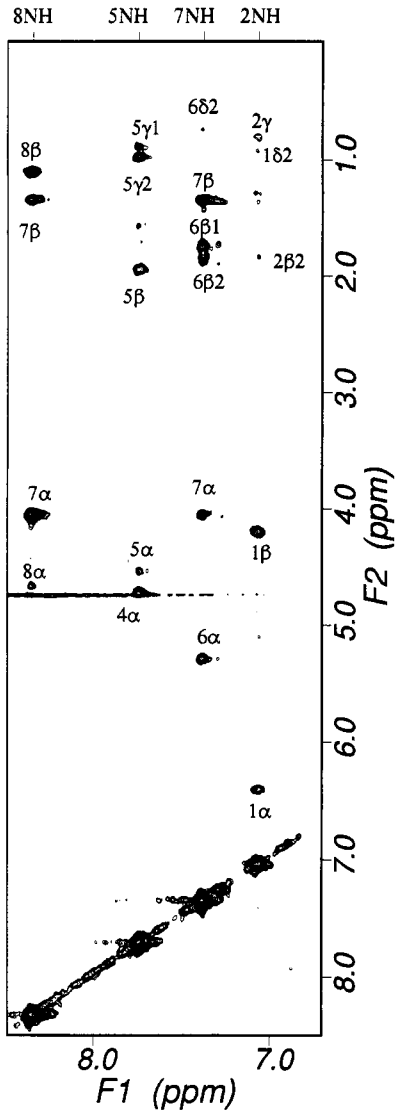

FIGURE 2: $^{15}N(\omega_2)$ half-filtered NOESY spectrum recorded using pulsed field gradients (Lee et al., 1993) with [U-^{15}N]CsA bound to unlabeled eCyP F112W (1 mM complex in 500 μL of a mixed solvent of 90% H_2O/10% D_2O, 50 mM sodium phosphate, and 0.04% sodium azide, pH 6.2, 25 °C, mixing time 50 ms). The region (ω_1 = 0.5–8.6 ppm, ω_2 = 6.6–8.6 ppm) that contains all the cross peaks of the $^{15}N(\omega_2)$ selected spectrum is shown. The chemical shift positions of the amide protons are indicated at the top of the spectrum.

CsA to other protons of CsA and *E. coli* cyclophilin. By editing in a third dimension by the ^{13}C frequencies in the 3D NMR experiment, many NOEs were well resolved and readily assigned. CsA/CsA and CsA/CyP NOEs were distinguished from one another by the presence or absence of diagonally related peaks. CsA/CsA NOEs were detected from both NOE partners at the two corresponding ^{13}C frequencies whereas CsA/CyP NOEs were only detected in one plane at the CsA ^{13}C frequencies. These NOEs were also distinguished in the $^{13}C(\omega_1,\omega_2)$ double-half-filtered NOESY spectrum where CsA/CsA cross peaks are detected in the $^{13}C(\omega_1,\omega_2)$ doubly selected subspectrum and CsA/CyP NOEs are observed in the $^{13}C(\omega_2)$-selected-$^{13}C(\omega_1)$-filtered subspectrum. For a qualitative interpretation of the 3D NOE data, NOE cross peaks were analyzed from the different ^{1}H-^{1}H 2D planes at the individual ^{13}C frequencies. For a semiquantitative interpretation of the 3D NOE data, 3D NOE cross-peak volumes were integrated in a spectrum with 50-ms mixing time. They were calibrated with respect to the known distance between the two α-methylene protons of Sar-3.

Table 2: ^{1}H and ^{13}C NMR Assignments of Cyclosporin A Bound to *E. coli* Cyclophilin F112W[a]

residue	assignment	^{1}H	^{13}C
MeBmt-1	NCH_3	3.20	36.45
	C=O		
	α	6.40	60.05
	β	4.20	
	γ		
	δCH_3	0.95	17.45
	δ		
	ε	5.50	
	ζ		
	η	1.75	19.25
Abu-2	NH	7.02	
	C=O		
	α	4.70	53.45
	β	1.36, 1.82	25.25
	γ	0.83	11.88
Sar-3	NCH_3	3.43	38.95
	C=O		
	α	3.76, 4.95	52.35
MeLeu-4	NCH_3	3.15	33.86
	C=O		
	α	4.76	58.15
	β	1.55, 1.70	38.15
	γ	1.48	25.7
	δ_1	0.84	23.95
	δ_2	0.60	22.55
Val-5	NH	7.70	
	C=O		
	α	4.55	57.35
	β	1.95	31.75
	γ_1	0.91	20.25
	γ_2	0.98	20.90
MeLeu-6	NCH_3	3.00	32.55
	C=O		
	α	5.30	56.75
	β	1.75, 1.82	38.15
	γ	1.46	25.75
	δ_1	0.95	24.95
	δ_2	0.75	21.25
Ala-7	NH	7.34	
	C=O		
	α	4.06	51.75
	β	1.32	19.05
D-Ala-8	NH	8.31	
	C=O		
	α	4.65	46.95
	β	1.08	17.55
MeLeu-9	NCH_3	2.50	31.05
	C=O		
	α	5.20	53.75
	β		
	γ	0.70	24.75
	δ_1	0.23	25.05
	δ_2	0.45	22.25
MeLeu-10	NCH_3	2.66	34.00
	C=O		
	α	5.65	55.55
	β	1.45	37.85
	γ	1.35	27.55
	δ_1	1.05	25.25
	δ_2	1.05	21.25
MeVal-11	NCH_3	2.19	33.45
	C=O		
	α	4.35	61.75
	β	1.40	26.05
	γ_1	0.25	21.55
	γ_2	−0.70	18.07

[a] Proton and carbon chemical shifts are referenced to TSP.

Supplementary constraints were obtained from the $^3J_{HN\alpha}$ coupling constants measured with a 2D version of a quantitative *J*-correlation H^NH^α experiment (Vuister & Bax, 1993). The resulting values for $^3J_{HN\alpha}$ and the derived φ-angle constraints were Val-5 ~ 5.3 Hz ($-50° > \phi > -170°$), Ala-7 ~ 3.5 Hz ($-40° > \phi > -90°$), and D-Ala-8 ~ 6.7 Hz ($60° < \phi < 160°$).

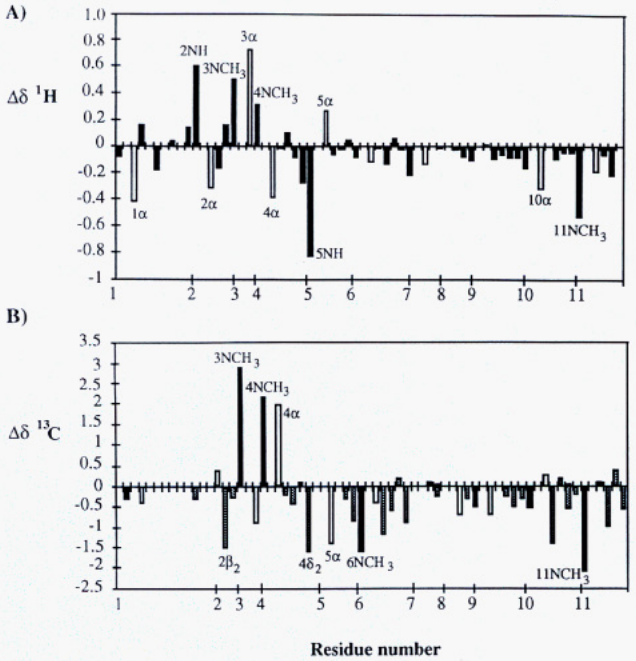

FIGURE 3: (A) ^{1}H chemical shift comparison of all the ^{1}H resonances in CsA when bound to eCyP F112W with those of CsA when bound to hCyPA. Chemical shifts of CsA bound to hCyPA (Fesik et al., 1991) were subtracted from the values listed in Table 2. The data are shown along the horizontal axis in the same order as listed in Table 2. The atoms for which significant differences are observed are indicated on the graph; empty bars represent H^α, and black bars represent all other ^{1}H atoms. (B) ^{13}C chemical shift comparison of all ^{13}C atoms in CsA when bound to eCyP F112W with those of CsA when bound to hCyPA. Chemical shifts of CsA bound to hCyPA (Fesik et al., 1991) were subtracted from the values listed in Table 2, which had been previously corrected to be referenced to dioxane. The atoms for which significant differences are observed are indicated on the graph; black bars represent methyl ^{13}C atoms attached to amide N, empty bars represent C^α, and dotted bars represent all other ^{13}C atoms.

The ϕ-angle constraints for D-alanine were obtained using a symmetry-related Karplus equation for D amino acids. Inital structure calculations were carried out using a simulated annealing protocol with NOE and ϕ-angle constraints only. This resulted in a rather well-defined backbone conformation. After this step, additional dihedral angle constraints were derived for some side chains in a similar way as described by Fesik et al. (1991). For Val-5 and MeVal-11 both H^α/H^γ NOEs are of similar intensity, and the H^α/H^β NOE is absent, indicating a χ^1 of 180°. Observation of the NOEs MeBmt^1-(NCH_3)/MeVal-11(H^{γ_1}) and MeVal-11(NCH_3)/MeVal-11-(H^{γ_2}) as well as the MeLeu-6(CH_3)/Val-5(H^{γ_1}) and Val-5(NH)/Val-5(H^{γ_2}) NOEs is consistent with this dihedral angle and provides stereospecific assignments of the methyl groups of Val-5 and MeVal-11. MeLeu-4 and MeLeu-6 show strong NCH_3/H^γ NOEs, consistent with a χ^1 of −60°. MeLeu-4, MeLeu-6, and MeLeu-9 have strong NOEs between the H^α and only one of its H^δ resonances. This is only compatible with a χ^2 of 180° and provides stereospecific assignments of the methyl groups of MeLeu-4, MeLeu-6, and MeLeu-9.

Structure of Bound CsA. Final structures were computed on the basis of 102 NOE distance (56 intraresidue, 29 sequential, and 17 others) and 10 dihedral angle constraints (3ϕ, $4\chi^1$, and $3\chi^2$). A total of 200 structures were calculated. From these structures, 18 were chosen that best satisfied the experimentally derived distance constraints and had the lowest NOE energy contribution (Figure 4). All of these structures agreed well with the experimental constraints, and there were no NOE violations greater than 0.3 Å. For these 18 structures the average rms deviation of the backbone atoms was 0.27 (±0.03) Å and for all heavy atoms was 0.48 (±0.05) Å. Average backbone and heavy atoms rms deviations per residue are shown in Figure 5A. Average dihedral angles Φ and Ψ and angular order parameters $S(\Phi)$ and $S(\Psi)$ (Hyberts et al., 1992) are shown in Figure 5B, and average dihedral angles χ^1 and χ^2 and angular order parameters $S(\chi^1)$ and $S(\chi^2)$ are shown in Figure 5C.

The conformation of CsA bound to eCyP F112W (Figure 4) contains no regular secondary structure. The two antiparallel backbone segments from residues 4 to 7 and 9 to 2 have their planar peptide bonds rotated out of the plane defined by the cyclic polypeptide backbone. The side chains of MeBmt-1, MeLeu-4, MeLeu-6, and MeLeu-10 are in front of the plane defined by the cyclic polypeptide backbone (Figure 4) and form a compact hydrophobic cluster. Side chains of Abu-2, Val-5, MeLeu-9, and MeVal-11 are behind this backbone plane. Some of the specific long-range NOEs that support this conformation include MeBmt-1(NCH_3)/Val-5(H^{γ_1}), MeBmt-1(NCH_3)/ MeLeu-6(NCH_3), MeBmt-1(H^η)/ MeLeu-4(NCH_3), MeBmt-1(H^η)/ MeLeu-6(H^{γ_2}), Val-

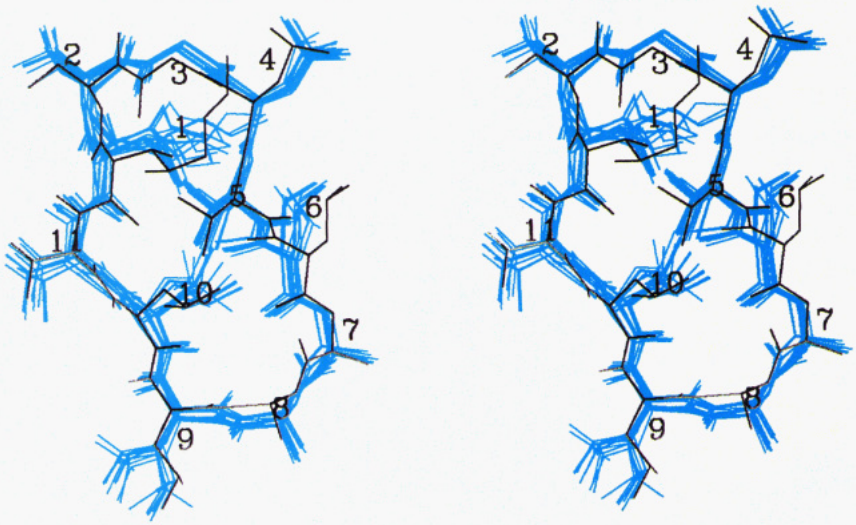

FIGURE 4: Stereo representation of the 18 best energy-minimized NMR-derived structures of CsA bound to eCyP F112W (blue) and the average NMR structure of CsA bound to hCyPA (black) (Fesik et al., 1991). All the structures were superimposed on the average structure of CsA bound to eCyP F112W.

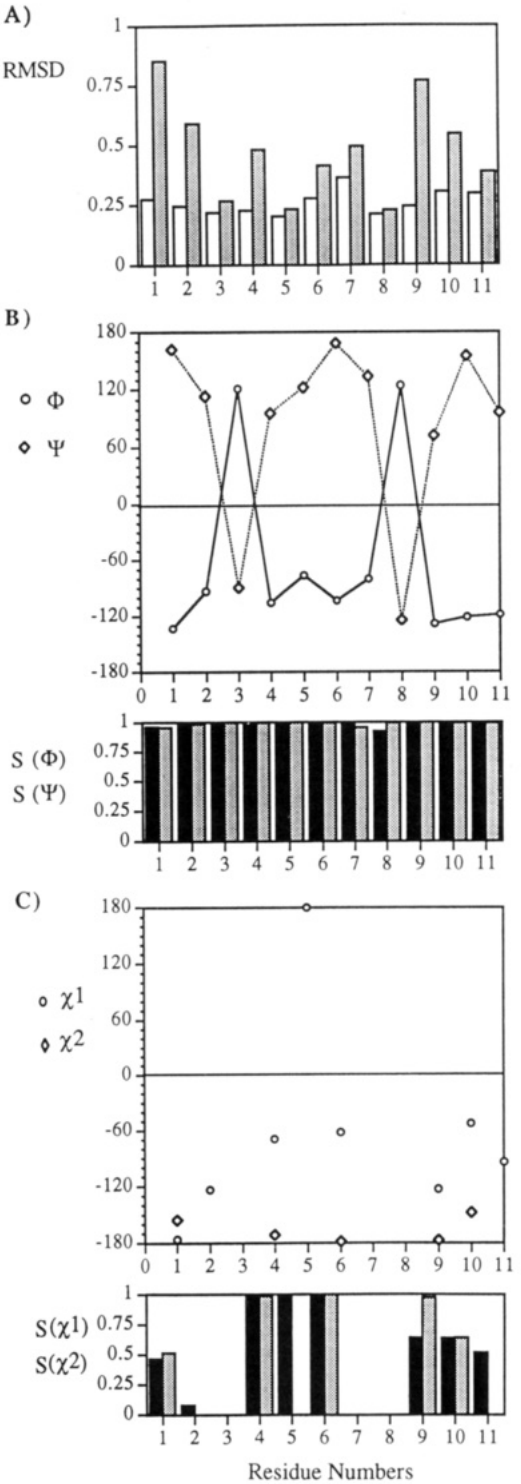

FIGURE 5: (A) Average rms displacements of the backbone atoms (N, C^{α}, C′) (empty bars) and all heavy atoms (dotted bars) from the average structure. The average structure was calculated by averaging the positions of the ensemble after the superposition of backbone atoms of 17 structures on the structure with the lowest pairwise rmsd values to the others. Backbone and heavy-atom root mean square deviations per residue were calculated for each structure superimposed on the average structure and then averaged over 18 structures. Average dihedral angles (B) Φ and Ψ and (C) χ^1 and χ^2. The angular order parameters $S(\Phi)$ (black bars) and $S(\Psi)$ (dotted bars) and $S(\chi^1)$ (black bars) and $S(\chi^2)$ (dotted bars) are shown at the bottom of the figures.

5($H^{\gamma 2}$)/Sar-3(NCH_3), Val-5($H^{\gamma 2}$)/MeLeu-10(NCH_3), MeLeu-6(NCH_3)/MeLeu-10(NCH_3), MeLeu-6(NCH_3)/MeLeu-10($H^{\delta 1}$), MeLeu-6($H^{\gamma 1}$)/MeBmt-1(H^{η}), and MeLeu-10(NCH_3)/MeBmt-1(NCH_3).

DISCUSSION

The structures of CsA in complex with hCyP and the eCyP F112W mutant were found to be virtually identical. Therefore, one might assume that the CsA binding sites in both proteins are identical. As will be discussed below, this is only true in part. One face of the CsA binding site in the eCyP mutant seems to have a substantially different architecture. This conclusion is drawn on indirect evidence. At this point, we have a solution structure of wild-type eCyP and of CsA bound to the eCyP mutant. However, the structure of the complex between CsA and the eCyP mutant has not yet been solved. Thus, the comparison of the binding sites is based on the structure of the wild-type eCyP. However, the structures of eCyP and hCyP are very similar in the region of Trp-121h[2] or Phe-112e, respectively, and the F112W mutation in eCyP is expected to result in nearly identical structures in this region. The differences are at the opposite end of the binding site, when the uncomplexed wild-type eCyP structure is compared with hCyP. One might argue that binding of CsA could induce a structural change in the protein. However, the structures of free hCyP (Ke et al., 1991) and hCyP in complex with CsA (Thériault et al., 1993; Pflügl et al., 1993) are very similar. Therefore, we think that the comparison described below is relevant.

Comparison of the CsA Binding Sites of hCyP and eCyP. While the X-ray structure of uncomplexed hCyP (Ke et al., 1991; Ke, 1992) and a number of X-ray and solution structures of complexes of hCyPA with CsA or peptide substrates (Ke et al., 1991, 1993, Kallen et al., 1991; Kallen & Walkinshaw, 1992; Spitzfaden et al., 1992; Pflügl et al., 1993; Weber et al., 1991; Fesik et al., 1991; Thériault et al., 1993) have been reported, the structure of wild-type eCyP has been solved only recently (Clubb et al., 1994). The overall fold of wild-type eCyP (Clubb et al., 1993, 1994) is similar to that of uncomplexed hCyP (Ke et al., 1991; Ke, 1992) and of hCyP complexed to CsA or substrates (Spitzfaden et al., 1992; Thériault et al., 1993). The protein cores are nearly identical while some surface loops have significantly different conformations.

Figure 6 shows ribbon diagrams of the structures of both proteins with the CsA binding site oriented toward the observer. There are a number of deletions when both proteins are compared (Clubb et al., 1994). Polypeptide segments that are deleted in the other protein are colored in yellow. In Figure 6B, regions of hCyP that have contact with CsA (Spitzfaden et al., 1992; Pflügl et al., 1993; Thériault et al., 1993) are colored in purple. Segments that are in homologous positions in eCyP (Figure 6A) are also colored in purple, except for the segment on the B4–B5 loop (Gly-72–Thr-73 in hCyP) which is clearly in a different position in the eCyP structure. Instead, two other residues, Phe-60e on the B4–B5 connecting segment and Tyr-149e on the H3–B8 loop, appear to take this place in eCyP and are thus shown in purple as well. To facilitate the following discussion, Figure 7A shows a superposition of the CsA binding site of the hCyP/CsA complex (Thériault et al., 1993) (red) and the aligned structure of wild-type eCyP (blue). Figure 7B shows the same binding site, with CsA as bound to hCyP (Thériault et al., 1993).

A comparison of the amino acids that contact CsA in hCyP and amino acids in homologous positions in wild-type eCyP, based on the structure of the CsA/hCyP complex, is provided

[2] Standard abbreviations are used for the amino acids. Sequence numbers followed by e or h represent the numbers in eCyP and hCyP, respectively.

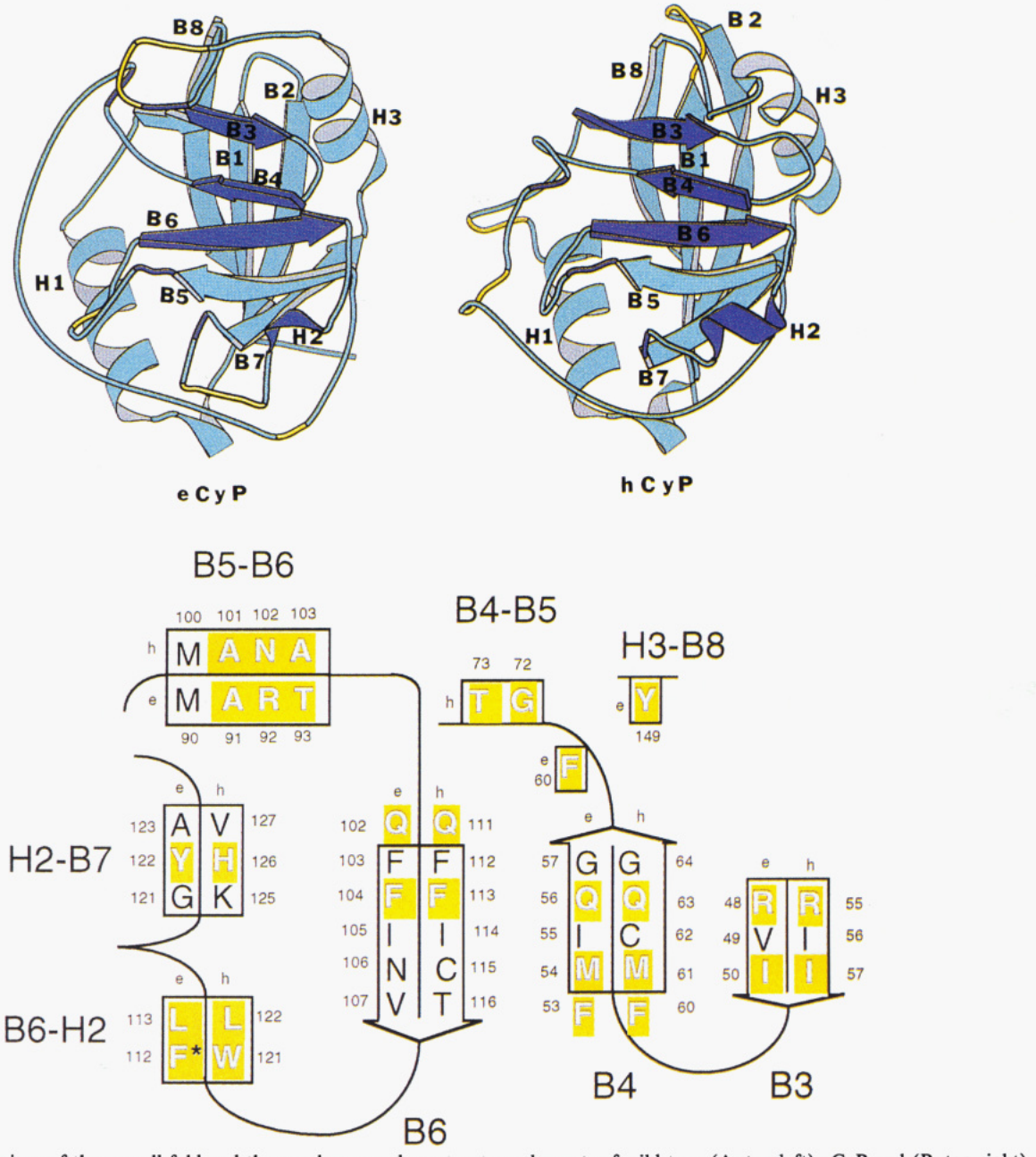

FIGURE 6: Comparison of the overall fold and the regular secondary structure elements of wild-type (A, top left) eCyP and (B, top right) hCyP (Clubb et al., 1994). The figure was produced with the program Molscript (Kraulis, 1991). The β-strands and helices are labeled B1–B8 and H1–H3, respectively. Regions that are deleted in the homologous protein are shown in yellow. Regions that contact CsA in hCyP and are proposed to contact CsA in eCyP are shown in purple. (C, bottom) Comparison of the amino acids of the CsA binding site. Residues that contact CsA in hCyP are shown in yellow. Residues that appear to be in equivalent positions in eCyP are shown in yellow as well. The residues of hCyP and eCyP are shown next to each other, and the respective sequence numbers are indicated on either side.

in Figure 6C. In hCyP, the CsA binding site is formed by three strands of β-sheets and four connecting segments (loops). The sequences of hCyP and eCyP are written next to each other and labeled with h and e, respectively. Residues that have direct contact with CsA in hCyP and corresponding residues in eCyP are marked in yellow. The residue F112 which is mutated in eCyP F112W is marked by an asterisk. The bottom of the elongated CsA binding pocket is formed by strands B4 and B6. The wall on one side of the binding pocket is rather flat. It is formed by strand B3. In hCyP, this wall is extended by the residues Gly-72h and Thr-73h of the B4–B5 loop. In the eCyP structure, this part of this wall is formed by the residues Phe-60e from the B4–B5 loop and Tyr-149e from the H3–B8 loop. The other wall of the binding pocket is somewhat steeper and is formed by the three loops B6–H2, H2–B7, and B5–B6. The residues forming the CsA binding site are rather well conserved between the two proteins, except for the part formed by the B4–B5 loop in hCyP. They are identical on the B3, B4, and B6 loops. On the B6–H2 loop, Leu-122h is identical, while Trp-121h is replaced with Phe-112e in wild-type eCyP. This is the key residue that is responsible for the lack of the CsA affinity in wild-type eCyP, which can be restored in the eCyP F112W mutant, as shown in this and a previous publication (Liu et al., 1991a). His-126h on the H2–B7 loop is replaced with Tyr-122e. Similarly, Asn-102h has only backbone contacts with CsA so that the replacement with Arg-92e should be conservative, as is the Ala-103h to Thr-93e exchange.

In the hCyP complex structure, Gly-72h and Thr-73h of the B4–B5 loop form contacts with the bound CsA. They are located on the upper rim of a twisted loop rising from the core of the protein toward the CsA binding site (Figure 7). The

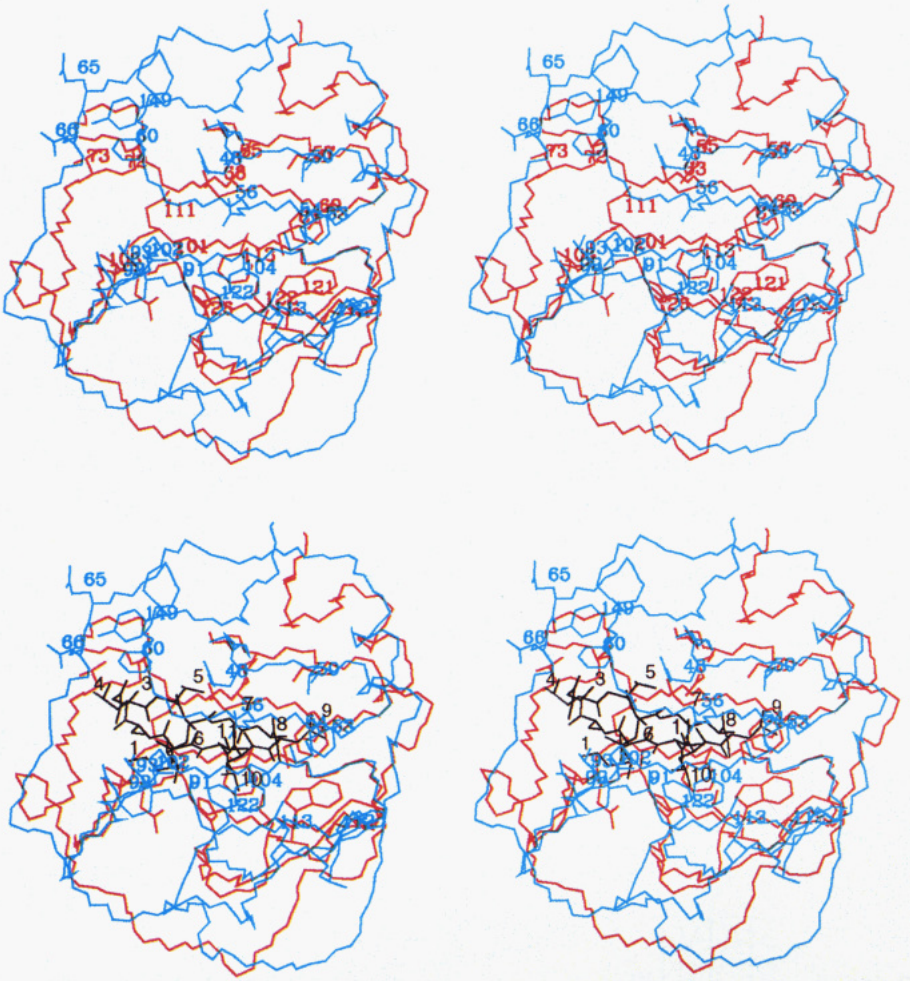

FIGURE 7: (A, top) Stereo representation of a superposition of the CsA binding site of hCyP as determined by NMR in the complex with CsA (red) (Thériault et al., 1993) and the corresponding site of uncomplexed wild-type eCyP (blue) (Clubb et al., 1994). Only side chains that appear to contact CsA are shown and identified with sequence numbers. (B, bottom) Same as (A), but the bound CsA is shown as determined by Thériault et al. (1993).

eCyP conformation of this segment is entirely different. The loop points away from the CsA binding site so that residues in positions homologous to Gly-72h and Thr-73h (Gln-65e and Gln-66e) are not expected to get in contact with CsA. However, the side chain of Phe-60e at the very beginning of the B4–B5 loop could take over the space of Gly-72h. In addition, the H3–B8 loop of eCyP, which is five residues longer than the corresponding loop in hCyP, is reaching out to this end of the binding pocket. Tyr-149e, located at the apex of this loop, together with the side chain of Phe-60e forms a hydrophobic wall that might stabilize bound CsA. Indeed, the CsA residues Sar-3 and MeLeu-4 show NOEs to aromatic eCyP resonances in the complex of the F112W mutant (see below).

The importance of Trp-121h has been discussed in the literature extensively. Together with Phe-60h, it encloses the CsA binding pocket on the right-hand side (Figure 7). The Trp-121 side-chain ϵNH group forms a H-bond to MeLeu-9(CO) of CsA. This H-bond cannot be formed with Phe-112e of eCyP. The eCyP F112W mutant binds CsA well, but still a factor of 10 weaker than hCyP (see Table 1). The reasons for this could be due to the fact that the side chain of Phe-112e in the structure of uncomplexed eCyP, and likely Trp-112 in the eCyP mutant, appears to be more remote from the CsA binding site than Trp-121h in both uncomplexed hCyP (Ke et al., 1991; Ke, 1992) and the hCyP/CsA complex (Thériault et al., 1993) (Figure 7). Additional reasons for the weaker binding could be sought in differences of other residues facing CsA such as His-126h, which is replaced with Tyr-122e. While previously a H-bond was proposed between the His-126(ϵNH) and MeVal-11(CO) (Spitzfaden et al., 1992), and claimed again in the recent X-ray structure of a pentameric CsP/CsA complex (Pflügl et al., 1993), the NMR structure of the complex shows evidence against this H-bond (Thériault et al., 1993). In the latter structure, however, a H-bond between the side chain of His-126h and Met-100h is shown which would have to be different in eCyP where His-126h is replaced with Tyr-122e. The difference in this position might cause a difference in the conformation of the B5–B6 loop, due to the altered interaction with Met-90e (Met-100h). The backbone NH and CO of Asn-102h form two hydrogen bonds with Abu-2(CO) and MeVal-11(CO) (Thériault et al., 1993), while the side chain of Asn-102h is not involved in direct contacts with CsA. The substitution of Asn-102h with Arg-92e should have only indirect effects on the CsA affinity (influencing the conformation of the H2–B7 and B5–B6 loops). The replacement of Ala-103h with Thr-93e should be conservative. The roles of Gly-72h and Thr-73h located in the long B4–B5 loop have been discussed above.

Intermolecular Contacts between CsA and eCyP F112W. While the contacts between CsA and hCyP are well characterized already, only rather limited information is available for the F112W eCyP complex with CsA, due to the lack of extensive mutant protein assignments. NOEs between CsA and eCyP F112W, observed in a (^{1}H,^{1}H)NOESY spectrum recorded with a ^{13}C(ω_1,ω_2) double-half-filter (Figure 8), were

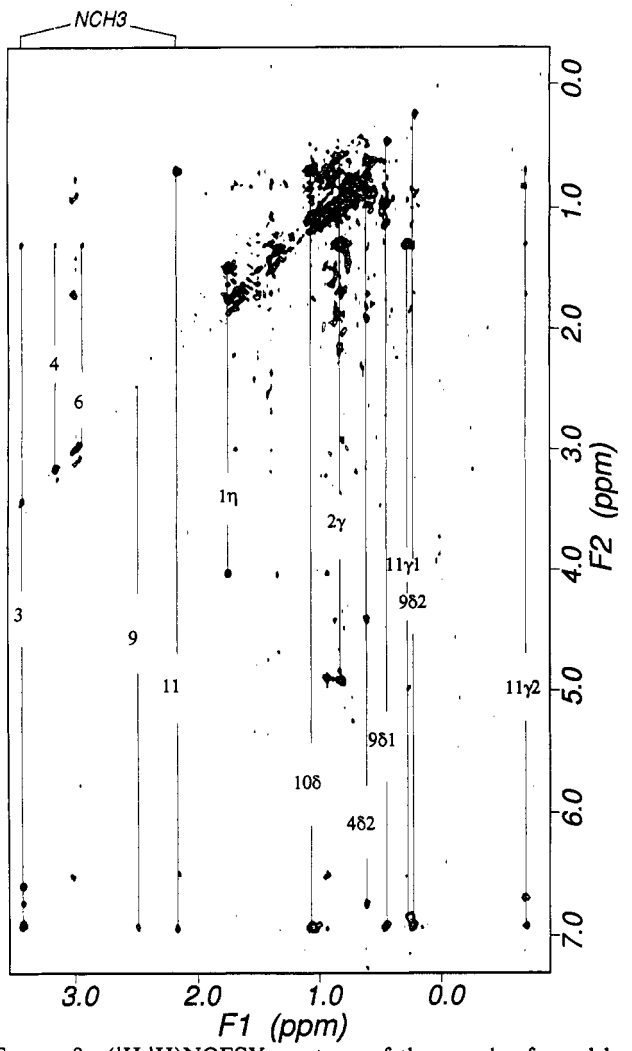

FIGURE 8: (^{1}H,^{1}H)NOESY spectrum of the complex formed by unlabeled eCyP F112W and [U-^{13}C]CsA recorded with a $^{13}C(\omega_1,\omega_2)$ double-half-filter. The $^{13}C(\omega_2)$-selected–$^{13}C(\omega_1)$-filtered subspectrum is shown (mixing time 50 ms; experimental conditions are the same as in Figure 1). Chemical shift positions of CsA resonances are indicated at the top of the spectrum.

used to identify those portions of CsA that interact with the protein. Figure 9 schematically depicts the CsA protons that are in close proximity to cyclophilin. Both $C^{\gamma}H_3$ groups of MeVal-11, MeVal-11(NCH_3), MeLeu-10(H^{δ_2}), both $C^{\delta}H_3$ groups of MeLeu-9, MeLeu-9(NCH_3), MeLeu-4(H^{δ_2}), and Sar-3(NCH_3) protons of CsA are all near aromatic as well as aliphatic protons of cyclophilin. The MeBmt-1(H^{η}), MeBmt-1(H^{δ}), and Abu-2(H^N) protons are not close to the aromatic but only to the aliphatic protons of cyclophilin.

From Figure 3 it is seen that there are large ^{1}H and ^{13}C chemical shift differences for resonances of residues Abu-2, Sar-3, Val-5, and MeVal-11 relative to CsA bound to hCyPA (Fesik et al., 1991), suggesting that the CyP binding pocket in the vicinity of these CsA residues is different in the two complexes. The chemical shift differences between CsA bound to hCyPA and CsA bound to eCyP F112W can be qualitatively rationalized from the information on intermolecular interactions. Since many of the intermolecular NOEs are with aromatic rings of CyP, chemical shift differences cannot have a clear trend toward high or low field (Figure 3), because both the sign and the magnitude of the ring current shifts depend on the relative orientation of the aromatic rings and the CsA protons. Overall, the CsA chemical shifts are similar for the part of CsA that is on the right-hand side in Figure 7. The

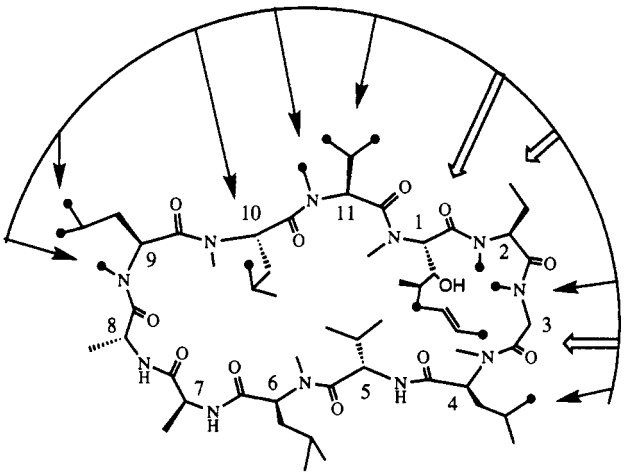

FIGURE 9: Primary structure of cyclosporin A. The filled circles indicate those CsA protons with NOEs to eCyP F112W as observed in the 3D HMQC-NOESY experiment and in the $^{13}C(\omega_2)$-selected–$^{13}C(\omega_1)$-filtered subspectrum of the $^{13}C(\omega_1,\omega_2)$ double-half-filtered NOESY experiment with a mixing time of 50 ms. Double arrows indicate NOEs to aliphatic resonances and single arrows indicate NOEs to both aliphatic and aromatic resonances of the protein.

largest chemical shift differences are for those residues that are close to the B4–B5 loop in hCyP which appears to be replaced by the two aromatic side chains of Tyr-149e and Phe-60e, consistent with what was discussed above in the comparison of the structure of uncomplexed wild-type eCyP and hCyP.

CONCLUSION

Previous studies on the periplasmic isoform of eCyP revealed that the protein has PPIase activity but low affinity for binding the immunosuppressive drug CsA. The eCyP F112W mutant was based on sequence alignment and the importance of the single tryptophan 121 in human CyPA for CsA binding (Liu et al., 1991b). In this work, we have analyzed CsA competitive inhibition of both wild-type and eCyP F112W and observed that the mutation to an indole side chain gives a 20-fold improvement in CsA binding as measured by PPIase K_i values. More interestingly, this 170 nM binding constant allows measurement of the ability of the eCyP F112W to present bound CsA for inhibition of the phosphatase activity of calcineurin. The eCyP F112W/CsA complex inhibits calcineurin with K_i = 1.1 μM, only 4-fold higher than the K_i value of 270 nM for hCyPA/CsA (Etzkorn et al., 1994) despite the wide divergence between the primary sequence of eCyP and hCyPA (34% identity).

This result has prompted us to determine by NMR methods the conformation of bound CsA to see how closely it resembles the drug bound to hCyPA. As one might have anticipated, the conformations of CsA bound to each CyP are indeed very similar. Chemical shift differences between CsA resonances for CsA bound to hCyPA and CsA bound to eCyP F112W and intermolecular NOEs between CsA and the protein indicate that there are differences in the structure of the binding pocket of hCyPA and eCyP F112W. The main differences have been localized at the B4–B5 loop which contacts CsA in hCyP with two residues; in eCyp this region adopts an entirely different conformation. Instead, Phe-60e at a different position of the B4–B5 loop and Tyr-149e from the much longer H3–B8 loop form this part of the CsA pocket in eCyP. Future structural studies of the eCyP F112W mutant in the CsA complex will allow further comparison with the hCyPA conformation, already well-defined by NMR (Thériault et

al., 1993) and X-ray (Pflügl et al., 1993). The extent to which various cyclophilins determine the efficacy of bound CsA presentation and calcineurin inhibition is an intriguing problem in defining the precise mode of action of cyclosporin A. Determination of the calcineurin-interacting surfaces of hCyPA and of eCyP should help to map out the crucial calcineurin immunophilin protein–protein recognition determinants.

ACKNOWLEDGMENT

We thank Dr. Hans Widmer (Sandoz, Basel) for providing ^{15}N- and ^{13}C-labeled cyclosporin A and Dr. Andrzej Krezel for assistance with the structure calculations.

REFERENCES

Bax, A., Clore, G. M., Driscoll, P. C., Gronenborn, A. M., Ikura, M., & Kay, L. E. (1990) *J. Magn. Reson. 87,* 620.

Bodenhausen, G., & Ruben, D. (1980) *Chem. Phys. Lett. 69,* 185–188.

Clubb, R. T., Thanabal, V., Fejzo, J., Ferguson, S. B., Zydowski, L., Baker, H. C., Walsh, C. T., & Wagner, G. (1993) *Biochemistry 32,* 6391–6401.

Clubb, R. T., Ferguson, S. B., Walsh, C. T., & Wagner, G. (1994) *Biochemistry 33,* 2761–2772.

Etzkorn, F. A., Chang, Z., Stolz, L. A., & Walsh, C. T. (1994) *Biochemistry* (in press).

Fesik, S. W., & Zuiderweg, E. R. P. (1988) *J. Magn. Reson. 78,* 588.

Fesik, S. W., Gampe, R. T., Jr., Eaton, H. L., Gemmecker, G., Olejniczak, E. T., Neri, P., Holzman, T. F., Egan, D. A., Edalji, R., Simmer, R., Helfrich, R., Hochlowski, J., & Jackson, M. (1991) *Biochemistry 30,* 6574–6583.

Fesik, S. W., Neri, P., Meadows, R., Olejniczak, E. T., & Gemmecker, G. (1992) *J. Am. Chem. Soc. 114,* 3165–3166.

Fischer, G., Wittmann-Liebold, B., Lang, K., Kiefhaber, T., & Schmid, F. X. (1989) *Nature 337,* 476–478.

Heald, S. L., Harding, M. W., Handschumacher, R. E., & Armitage, I. M. (1990) *Biochemistry 29,* 4466–4478.

Hsu, V. L., & Armitage, I. M. (1992) *Biochemistry 31,* 12778–12784.

Hyberts, S. G., Goldberg, M. S., Havel, T. F., & Wagner, G. (1992) *Protein Sci. 1,* 736–751.

Kallen, J., & Walkinshaw, M. D. (1992) *FEBS Lett. 300,* 286–290.

Kallen, J., Spitzfaden, C., Zurini, M. G. M., Wider, G., Widmer, H., Wüthrich, K., & Walkinshaw, M. D. (1991) *Nature 353,* 276–279.

Ke, H. (1992) *J. Mol. Biol. 228,* 539–550.

Ke, H., Zydowsky, L. D., Liu, J., & Walsh, C. T. (1991) *Proc. Natl. Acad. Sci. U.S.A. 88,* 9483–9487.

Ke, H., Mayrose, D., & Cao, W. (1993) *Proc. Natl. Acad. Sci. U.S.A. 90,* 3324–3328.

Kessler, H., Köck, M., Wein, T., & Gehrke, M. (1990) *Helv. Chim. Acta 73,* 1818–1832.

Kofron, J. L., Kuzmic, P., Kishore, V., Gemmecker, G., Fesik, S. W., & Rich, D. H. (1992) *J. Am. Chem. Soc. 114,* 2670–2675.

Kraulis, P. (1991) *J. Appl. Crystallogr. 24,* 946–950.

Lee, J., Fejzo, J., & Wagner, G. (1993) *J. Magn. Reson. B 102,* 322–325.

Liu, J., & Walsh, C. T. (1990) *Proc. Natl. Acad. Sci. U.S.A. 87,* 4028–4032.

Liu, J., Chen, C.-M., & Walsh, C. T. (1991a) *Biochemistry 30,* 2306–2310.

Liu, J., Farmer, J. D., Jr., Lane, W. S., Friedman, J., Weissman, I., & Schreiber, S. L. (1991b) *Cell 66,* 807–815.

Neri, P., Gemmecker, G., Zydowsky, L. D., Walsh, C. T., & Fesik, S. W. (1991) *FEBS Lett. 290,* 195–199.

Nilges, M., Clore, G. M., & Gronenborn, A. M. (1988) *FEBS Lett. 239,* 129–136.

Otting, G., & Wüthrich, K. (1988) *J. Magn. Reson. 76,* 569–574.

Otting, G., & Wüthrich, K. (1990) *Q. Rev. Biophys. 23,* 39–96.

Pflügl, G., Kallen, J., Schirmer, T., Jansonius, J. N., Zurini, M. G. M., & Walkinshaw, M. D. (1993) *Nature 361,* 91–94.

Spitzfaden, C., Weber, H.-P., Braun, W., Kallen, J., Wider, G., Widmer, H., Walkinshaw, M. D., & Wüthrich, K. (1992) *FEBS Lett. 300,* 291–300.

Thériault, Y., Logan, T. M., Meadows, R., Yu, L., Olejniczak, E. T., Holzman, T. F., Simmer, R. L., & Fesik, S. W. (1993) *Nature 361,* 88–91.

Vuister, G., & Bax, A. (1993) *J. Am. Chem. Soc. 115,* 7772–7777.

Weber, C., Wider, G., von Freyberg, B., Traber, R., Braun, W., Widmer, H., & Wüthrich, K. (1991) *Biochemistry 30,* 6563–74.

Zydowsky, L. D., Etzkorn, F. A., Chang, H., Ferguson, S. B., Stolz, L. A., Ho, S. I. & Walsh, C. T. (1992) *Protein Sci. 1,* 1092–1099.